Nationaal Lucht- en Ruimtevaartlaboratorium
National Aerospace Laboratory NLR

NLR-TP-2001-001

Pulsating & oscillating heat transfer devices in acceleration environments from microgravity to supergravity

A.A.M. Delil

Nationaal Lucht- en Ruimtevaartlaboratorium
National Aerospace Laboratory NLR

NLR-TP-2001-001

Pulsating & oscillating heat transfer devices in acceleration environments from microgravity to supergravity

A.A.M. Delil

This report concerns work done during a five months stay as a visiting professor at the Institute of Space and Astronautical Science, Sagamihara, Japan. It was presented as SAE-2001-02-2240 during the Two-Phase Technology 9B Session at the 31st Conference on Space Environmental Systems, Orlanda, USA, July 2001.

Division:	Space
Issued:	29 June 2001
Classification of title:	Unclassified

Contents

(18 pages in total)

2001-01-2240

Pulsating & Oscillating Heat Transfer Devices in Acceleration Environments from Microgravity to Supergravity

A.A.M. Delil
National Aerospace Laboratory NLR, The Netherlands

ABSTRACT

The work described was done during a five months stay as visiting professor at the Institute of Space and Astronautical Science, in Sagamihara, Japan. The research concentrates on pulsating and oscillating heat transfer devices, being of interest for applications in spacecraft thermal control in microgravity, in planetary partial gravity and hypergravity environment, and hypergravity acceleration levels in rotating spacecraft. Different aspects of various heat transfer devices in gravity environments ranging from micro-gravity to super-gravity are discussed. An overview is given of worldwide activities on and the state of the art of pulsating and oscillating heat transfer devices, in an attempt to assess commonalities and differences. Following the outcomes of this assessment, a baseline philosophy for modelling and for comparison of experimental data was defined, in order to anticipate an easy comparison with the results of ongoing and future research activities.
In addition a versatile test set-up was defined and developed such that it allows the variation of almost all the relevant parameters. The latter parameters are: Working fluid and fill charge, power, transport length, inclination with respect to the gravity vector, and the possibility to choose either the dead-end pulsating or the closed-loop oscillating configuration.

INTRODUCTION & BACKGROUND

NLR publications of the last decade discuss thermal-gravitational modelling & scaling of two-phase heat transport systems for spacecraft applications (Refs. 1 to 14). The initial research focused on mechanically and capillary pumped two-phase loops for use in micro-gravity. The activities dealt with pure geometric, pure fluid to fluid, or hybrid (combined) scaling of a prototype system by a model at the same gravity level, and of a prototype in micro-g by a model on earth. The scaling approach was based on dimension analysis and similarity considerations. The scaling research was later extended to applications for Moon and Mars bases. The research was done for a better understanding of the impact of gravitation level on two-phase flow and heat transfer phenomena, to provide means for comparison and generalisation of data, and to develop useful tools to design space-oriented two-phase systems and components based on the outcomes of terrestrial tests, and to save money by reducing costs.

Scaling to super-gravity levels was started a couple of years ago, as promising hyper/super-gravity applications for two-phase heat transport systems were identified: Thermal control systems for hyper-gravity planetary environment and cooling of high power electronics in spinning satellites (and in military aircraft, where during manoeuvres the electronics can be exposed to transient accelerations up to 120 m/s^2, 12 g). Experimental investigation of the high-g performance of two-phase heat transport loops was also started elsewhere (Refs. 17 to 20). The aforementioned overview of the NLR publications includes all relevant issues on the scaling approach, similarity considerations, useful equations, flow patterns issues, and scaling of “classical” (capillary) pumped two-phase loops between high acceleration levels, earth gravity, reduced gravity and micro-gravity, including against-(super-)gravity mode performances.

Two pulsating/oscillating two-phase heat transfer devices (HTD) can be distinguished: Pulsating two-phase heat transfer loops and novel devices, called e.g. pulsating heat pipe, looped heat pipe, spaghetti heat pipe, meandering heat pipe or flat swinging heat pipe. These systems have in common that the operation is driven only by vapour pressure (hence temperature) differences induced by the heat to be transported. They don’t need an additional power source. Fig. 1 depicts the temperature dependent saturation pressure of some candidate working fluids. It illustrates that when designing such devices, one has to select a fluid with a high saturation pressure gradient (dp/dT) in the operating (temperature) range, as the higher system pumping pressures correspond with higher dp/dT.

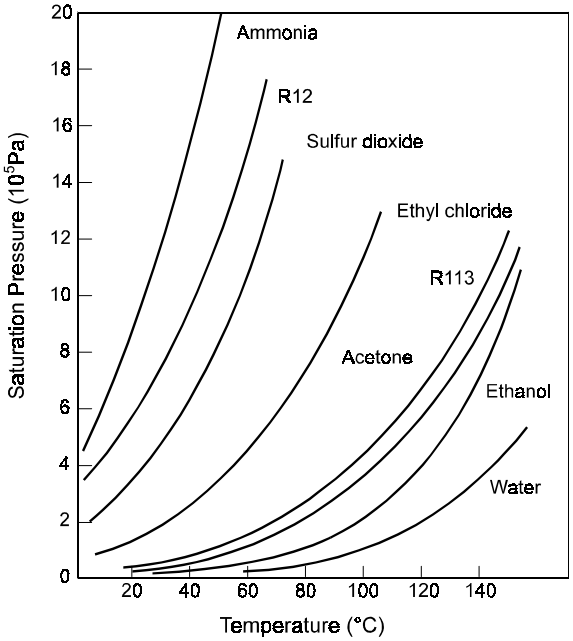

Figure 1. Saturation pressure versus temperature for various working fluids

PULSATING TWO-PHASE LOOPS

Pulsating two-phase heat transport loops (Fig. 2) and heat pipes (Fig. 3) were already proposed and tested in Europe in 1978 by Tamburini (Ref. 18). Similar devices were more recently studied by Lund in the US (Ref. 19) and in Russia by Borodkin (Ref. 20). These systems are just two-phase loops driven by vapour pressure differences, instead of mechanical or capillary pumping action. The vapour pressure pumping action is realised by incorporating in a normal loop) two one-way valves: one at the entrance, the other at the exit of any evaporator (Fig. 4). Power fed to the system increases the internal vapour pressure in the section between the two valves till the exit valve will open and the loop starts to run, also opening the second valve to let sub-cooled liquid flow into the pumping section. After some pressure decay the valves will close re-starting the process. A careful design will certainly lead to a properly performing heat transfer device.

Advantages of such loops are the driving mechanism (heat is being transferred without additional power source), high heat transport capability, self-priming capability and capability to work against gravity. A disadvantage is the pulsating operation, as pulsating heat and mass transfer, accompanied by temperature variations and possibly also vibrations (g-jitter) will make the system not attractive for some micro-gravity applications.

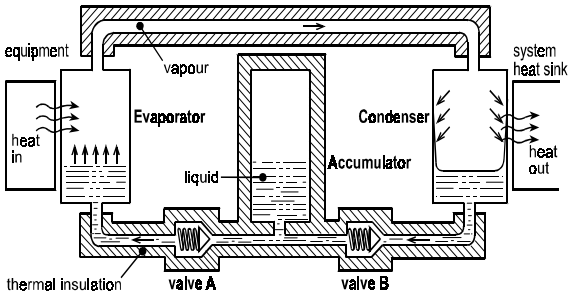

Figure 2. Tamburini's T-system pulsating loop concept

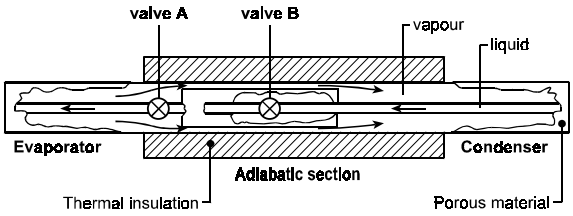

Figure 3. T-system derived pulsating heat pipe

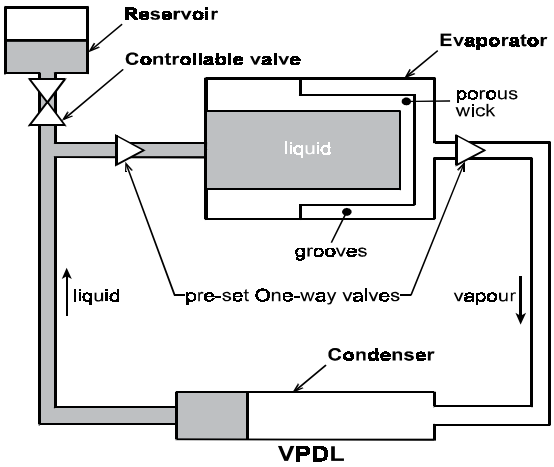

Figure 4. VPDL: vapour pressure driven loop

NOVEL HEAT PULSATING/OSCILLATING HEAT TRANSFER DEVICES

Novel oscillating and pulsating devices have many fancy names, like bubble-driven heat transfer device (Ref.21), oscillation controlled HTD (Ref. 22), pulsating or meandering heat pipe (Refs. 22, 23), looped capillary heat pipe or capillary tunnel heat pipe (Refs. 24, 25), flat swinging heat pipe (Ref. 26), and spirally wound or serpentine-like heat pipe (Ref. 27). Fig. 5 shows a schematic of a section of such a device, called looped (Ref. 28) or closed-loop (Ref. 22) if the two legs at each end are not dead ends but interconnected, creating a closed loop configuration. If

the latter configuration has a spring-like geometry like the arrangement discussed in the Refs. 28 and 29, the operation of the device has been frequently observed to stabilise after a certain start-up period, producing a periodic pumping of almost constant frequency into one direction (Ref. 29). Such behaviour is very similar to the behaviour of the pulsating heat transfer loops. This similarity suggests that the function of valves in the pulsating heat transfer loops is now delivered by stick-slip conditions of the slug-plug distribution of the working fluid in the closed- loop spring-like meandering structure, whose heating and cooling sections have also a certain periodicity. Anyhow, the slug-plug distribution is essential for these oscillating devices, which can be equipped with or without valves.

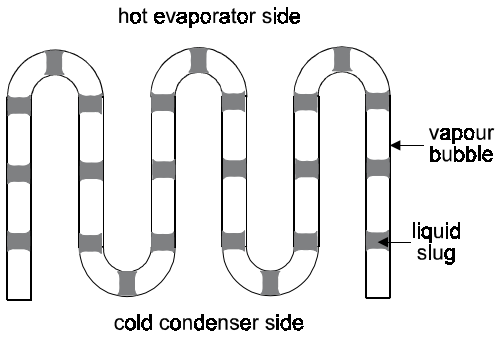

Figure 5. Schematics of a meandering heat pipe

TABLE 1. Relevance of π-numbers for thermal-Gravitational scaling of two-phase loops	Liquid Sections		Evaporator Swirl & Capillary	Vapour & 2-Phase Sections	Condenser
	Adiabatic	Heating/Cooling			
π_1 = D/L = geometry	•	•	•	•	•
$\pi_2 = Re_l = (\rho vD/\mu)_l$ = inertia/viscous	•	•	•	•	•
$\pi_3 = Fr_l = (v^2/gD)_l$ = inertia/gravity	•	•	•	/•	•
$\pi_4 = Eu_l = (\Delta p/\rho v^2)_l$ = pressure head/inertia	•	•	•	•	•
π_5 = cos ν = orientation with respect to g	•	•	•	/•	•
π_6 = S = slip factor = v_v/v_l			•	•	•
π_7 = density ratio = ρ_v/ρ_l			•	•	•
π_8 = viscosity ratio = μ_v/μ_l			•	•	•
$\pi_9 = We_l = (\rho v^2 D/\sigma)_l$ = inertia/surface tension		•	•	/•	•
$\pi_{10} = Pr_l = (\mu Cp/\lambda)_l$		•	•		•
$\pi_{11} = Nu_l = (hD/\lambda)_l$ = convection/conduction			•		•
$\pi_{12} = \lambda_v/\lambda_l$ = thermal conductivity ratio			•		•
$\pi_{13} = Cp_v/Cp_l$ = specific heat ratio		•	•	•	•
$\pi_{14} = \Delta H/h_{lv}$ = Boil =enthalpy nr. = X = quality			•	/•	•
$\pi_{15} = Mo_l = (\rho_l \sigma^3/\mu_l^4\, g)$ = capillarity/buoyancy			•	•	•
$\pi_{16} = Ma = v/(\partial p/\partial \rho)_s^{1/2}$			•		•
$\pi_{17} = (h/\lambda_l)(\mu_l^2 g)^{1/3}$					
$\pi_{18} = L^3 \rho_l^2\, g\, h_{lv}/\lambda_l \mu_l (T-T_o)$					

The velocities of bubbles and slugs in a tube are governed by buoyancy, liquid inertia, liquid viscosity and surface tension forces, in the general case of bubbly or slug-plug flow in a gravity field. This means that properly chosen dimensionless groups can be very helpful to discuss the aspects of slug-plug flow in oscillating devices (Ref. 30). The groups can be used together with the groups shown in Table 1 and in the Figs. 6 and 7, taken from dimension-analytical considerations discussed in the aforementioned overview articles and their references (Refs. 1-14, 31).

The condition of slug-plug distribution determines the maximum inner capillary tube diameter (Refs. 30, 32, 33) to be

$$d_{max} = 1.836\, g^{-1/2}\, [\sigma/(\rho_l - \rho_v)]^{1/2} \approx 1.836\, g^{-1/2}\, (\sigma/\rho_l)^{1/2}\,, \quad (1)$$

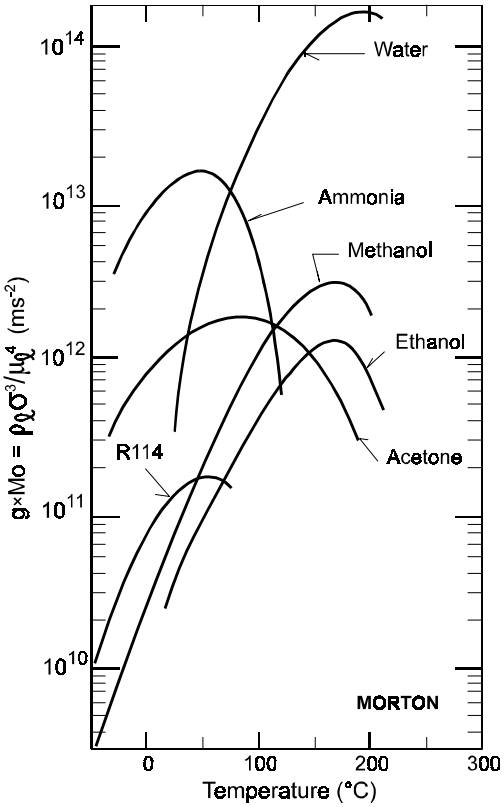

Figure 6. $\rho_l.\sigma^3/\mu_l^4$ versus temperature for six fluids

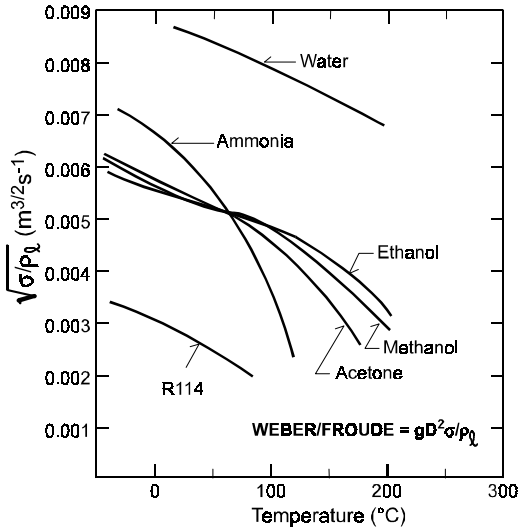

Figure 7. $(\dot{u}/\rho_l)^{1/2} = D.g^{1/2}/(We/Fr)^{1/2}$ versus temperature

for $\rho_l >> \rho_v$. Hence the thermal-gravitational scaling of the inner tube diameter can be derived from Fig. 7.

The slug-plug condition also sets the lower limit of the slug (bubble) size: It shall be at least 0.6 times the tube diameter (Refs. 30, 32, 33). This extra requirement has an impact on the liquid filling ratio $(1 - \alpha)$. If not fulfilled, the bubbles will be too small to maintain the slug flow pattern, characterised by high heat transfer densities. The resulting bubbly flow leads to a far less efficient heat transport.

Alternative useful plots of dimensionless numbers (Ref. 30) are shown in the Figs. 8 and 9. Fig. 8 depicts the dimensionless velocity v* as a function of Morton number Mo (see Table 1) and Eötvös Eö or Bond number Bo:

$$v^* = v\,[g\,d\,(1 - \rho_v/\rho_l)]^{-1/2} \approx v / (g\,d)^{1/2}, \qquad (2)$$

$$Eö = 4\,Bo = We/Fr = g\,d^2\,(\rho_l - \rho_v)/\sigma \approx g\,d^2\,\rho_l/\sigma. \qquad (3)$$

Fig. 9 depicts experimental data in the alternative plotting (Ref. 30): v* as a function of the inverse viscosity number Mu, for different values of Archimedes number Ar. The dimensionless numbers Mu and Ar are given by:

$$Mu = \mu_l\,[g\,d^3\,(\rho_l - \rho_v)\,\rho_l]^{-1/2} \approx \mu_l\,(g\,d^3\,\rho_l^2)^{-1/2}, \qquad (4)$$

$$(Ar)^2 = Mo = (\rho_l\,\sigma^3/\mu_l^4\,g) / (1 - \rho_v/\rho_l] \cong \rho_l\,\sigma^3/\mu_l^4\,g\,. \qquad (5)$$

The three asymptotes shown are: v* = 0.345 for Eö > 100 and $Mu < 10^{-3}$ (the inertia dominant domain), v*. Mu = 10^{-2} for Eö > 100 and Mu > 0.5 (the viscosity dominant domain), and Mu^2. Ar = 0.16 and Eö < 3.37 (the surface tension dominant domain). The last domain is the most important for the oscillating devices considered here, as Eö < 3.37 straightforwardly leads to the maximum tube diameter (equation 1) and dominating surface tension means that plug-slugs do not move, if there is no (thermal) power input. In this domain slug flow is guaranteed by surface tension, if slug bubbles have diameters of at least 0.6 times the tube diameter.

Some quantitative considerations on these pulsating two-phase heat transfer devices are presented later on, in order to get a certain feeling for or a better understanding of how to design, scale and test such devices. Geometrical data and some performance figures of the in the next chapter described single-phase oscillating heat transfer device will be used.

Anticipating later sections it is already remarked that the advantages of PHPs/OHPs as compared to normal heat pipes are: The problemless starting and restarting, the insensitivity for non-condensible gases, and relatively low production costs. Drawbacks are their sensitivity to puncture (one single puncture destroys the entire system), and their lower thermal

conductivity and inherent non-isothermal operation. However, these systems are proven to be attractive for applications in high gravity (acceleration) environments (Refs. 15, 26).

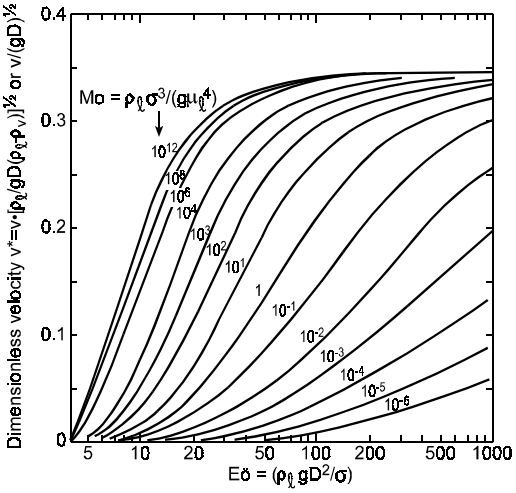

Figure 8. Dimensionless velocity v* as a function of the Morton number Mo and the Eötvös number Eö

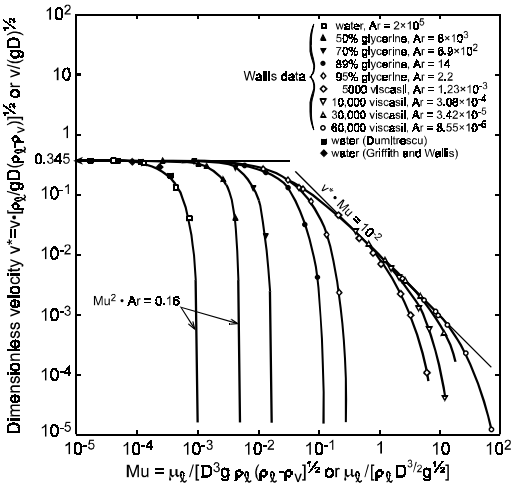

Figure 9. Experimental dimensionless velocity v* data as a function of dimensionless inverse viscosity Mu

A SINGLE-PHASE HEAT TRANSFER DEVICE AS THE BASELINE TO COMPARE DATA

Single-phase oscillating heat transport devices are discussed here, as not only the modelling of these devices is very useful to understand the operation of pulsating and oscillating heat pipes. Such a single-phase oscillating heat transfer device, depicted in Fig. 10, can namely be used as a baseline to compare experimental results of pulsating/oscillating heat pipes.

Detailed discussions on this synchronised forced oscillatory flow heat transfer device are given in the publications of the originators (Refs. 34 to 36) and in other publications on this device (Refs. 21, 23, 38, 39), respectively on related phase-shifted forced oscillatory flow heat transfer devices (Refs. 21, 23).

The set-up consists of two reservoirs at different temperatures, connected by a 0.2 m long, 12.7 mm inner diameter acrylic tube, containing 31 glass capillaries with an inner diameter d = 1 mm. The open cross-sectional area of the capillary structure, including the triangular sections between the capillaries, A_l was determined to be 67 mm^2, being 53% of the total inner cross-sectional area of the tube (A = 127 mm^2). The reservoirs are equipped with flexible membranes. A variable frequency shaker is used to oscillate the incompressible working liquid inside the capillary structure. Frequency f is variable from 2 and 8 Hz. The tidal displacement Δz is variable from 20 and 125 mm.

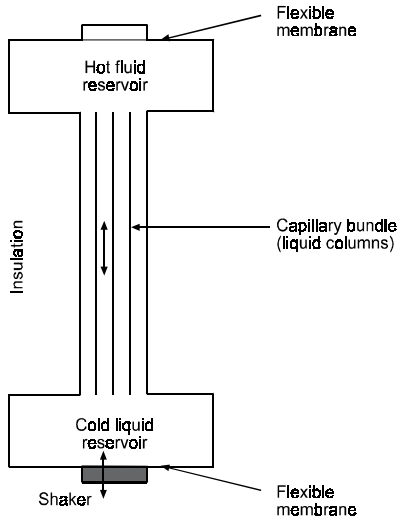

Figure 10. Synchronised forced oscillatory flow HTD

The operation is as follows. Starting with the capillary structure filled with hot liquid, this liquid is replaced, in the first half of the oscillation period, by liquid from the cold reservoir, except the thin (Stokes) boundary layer. Heat is then exchanged very effectively in radial direction between the hot Stokes layer and the cold

core. Heat accepted by the core is removed to the cold reservoir in the second half of the oscillation period. The heat flow, via the liquid, between the reservoirs is

$$Q = \lambda_{eff} (A_l/L)\, \Delta T = \rho_l\, Cp_l\, \kappa_{eff}\, (A_l/L)\, \Delta T. \quad (6)$$

ΔT is the temperature difference between hot and cold reservoir. κ_{eff} is the effective thermal diffusivity , λ_{eff} is the effective thermal conductivity.

Fig. 11 shows the experimentally determined effective thermal diffusivity as a function of tidal displacement and oscillation frequency, for a device with glass capillaries and water as working fluid. The solid lines are analytical predictions from the laminar theory. The figure indicates that the effective thermal conductivity via the liquid is

$$\lambda_{eff} = B\, \rho_l\, Cp_l\, \{(\Delta z)^2 / (d/2)\}\, (2\pi f\, \mu_l/\rho_l)^{1/2}. \quad (7)$$

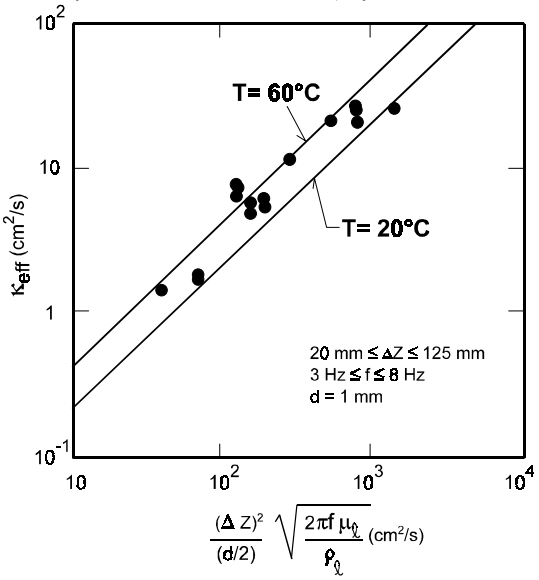

Figure 11. Effective thermal diffusivity

The proportionality factor B, the tangent of the straight lines in Fig. 11, can be written as (Refs. 34, 35):

$$B = 2^{-5/2}\, Pr_l^{-1} \{B' + B'' - B'B''\, (1 + Pr_l^{1/2}) * \\ * \{Pr_l^{-1/2} - 2\, (1 + Pr_l)\})\}. \quad (8)$$

$$B' = Pr_l/(Pr_l - 1) \text{ and } B'' = \{(1 - B')\, (Pr_l\, \kappa_l / \kappa_{wall})^{1/2} + \\ - B'\, \lambda_f / \lambda_{wall})\} * \{\lambda_f / \lambda_{wall} + (\kappa_l / \kappa_{wall})^{1/2}\}^{-1}. \quad (9)$$

An important conclusion for future design activities can be drawn by considering equations (6) to (9): Highest values of proportionality factor B occur for small Prandtl number and well thermal conductors walls (Ref. 35).

An alternative representation is obtained by defining an enhancement (proportionality) factor E for undeveloped oscillating flow in synchronised systems

$$(\lambda_{eff} / \lambda_f) - 1 = (\kappa_{eff} / \kappa_l) - 1 = (Pr_l\, \Delta z / 2d)^2\, E. \quad (10)$$

E depends on the dimensionless Womersley number (like the Schmidt number for axial contamination propagation and for pulmonary ventilation)

$$Wo_l = (d/2)\, (2\pi f\, \rho_l / \mu_l)^{1/2}. \quad (11)$$

$E = Wo_l^4 / 24$ for $Wo_l << 1$, and
$E = Wo_l\, (Wo_l - 2^{-1/2})$, for $Wo_l << 1$. (12)

Fig. 12 shows the enhancement factor E as a function of Womersley number, for decades of the Prandtl number: 0.1, 1 and 10 (Refs. 35, 37).

Inserting the properties of water at 293 K (20 °C), d = 1 mm, Δz = 125 mm and f = 8 Hz (hence Pr_l = 6.9 and Wo_l = 3.55), yields (according to figure 3) for the above synchronised device an enhancement factor 0.14. The corresponding λ_{eff} (about $1.2 * 10^4$ W/m.K) means a power density slightly above $3 * 10^6$ W/m^2. This is confirmed by the experimental data: $2.9 * 10^6$ W/m^2 for a gradient of 280 K/m (Ref. 34). The total effective thermal conductivity is roughly 5000 W/m.K, if based on the total cross-sectional tube area, including insulating glass walls.

A similar expression has been derived for undeveloped oscillating flow in phase-shifted systems (Ref. 21):

$$\lambda_{eff} = \lambda_f \{1 + 0.707\, (1 + Pr_l^{-1})^{-1}\, (1 + Pr_l^{-1/2})^{-1}\} * \\ * \{(\Delta z)^2/(d/2)\}\{(2\pi f\, \rho_l\, Cp_l/\lambda_f)^{1/2}\}. \quad (13)$$

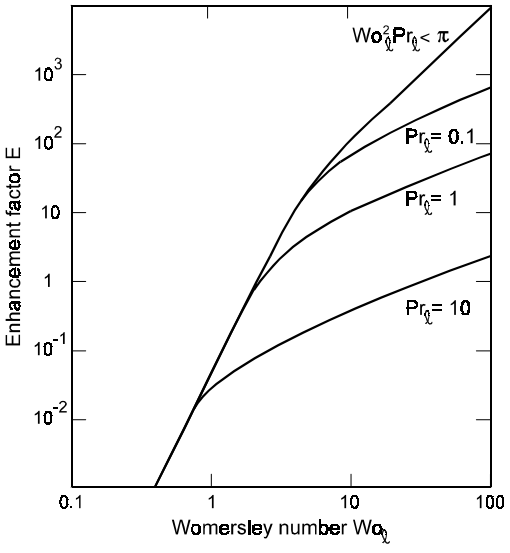

Figure 12. Enhancement factor E versus Wo and Pr

Inserting again the properties of water at 293 K, d = 1 mm, Δz = 125 mm and f = 8 Hz yields λ_{eff} = $2.5*10^4$ W/m.K, being 2.5 times the value of the corresponding synchronised forced oscillatory flow HTD.

Disadvantages of the concepts are poor current state of the art and power consumption of the shaker. The latter, more than 5 W in the described cases, strongly increases with oscillation frequency and tidal displacement. Disadvantage for some micro-gravity applications is the noise introduced by the shaker.

The major advantage of the concepts is their variable conductance, which is adjustable via the frequency and tidal displacement from almost zero (liquid in rest in a poorly conductance structure) to values comparable to or even better than heat pipes. This makes such devices very useful for instance to drain huge amounts of thermal power from a hot vessel for nuclear reactor cooling, in an emergency case.

Anticipating the section on the definition of the future testing approach, it is remarked that the above equations and the corresponding figures straightforwardly can be transformed to other single-phase oscillating devices using different working fluids, and having different capillary diameters, cross-sections, lengths and tidal displacements, etc. Consequently these transformations can be used to properly interpret the experimental outcomes of the novel oscillating and pulsating two-phase heat transfer devices discussed.

REVIEW OF THE MOST RELEVANT PHP & OHP PUBLICATIONS

The information is summarised in Table 2 below, is obtained from an overview of the abstracts of the most relevant publications on the subject (Refs. 15, 21, 22, 26, and 41 to 59), as it is given (including brief personal comments) in the appendix of reference 66.

When looking at this table and the contents of the corresponding references, it can be concluded that:

- The majority of the experiments do not constitute a good basis for a systematic approach. Up to know the overall picture looks rather random and chaotic (except for the work presented in the references 42 to 45, 48, 21, 15, 54 and 55). Co-ordination, being completely absent, is to be realised soon possible.
- The results of the most promising theoretical papers (refs. 45, 46) suggest that a critical combination of the two models and model equations, some adaptations and additions, will lead to an improved model which properly describes OHP/PHP behaviour, thus making the understanding of their operation much clearer.
- Fill charges below 30 % and above 80 % are to be avoided, as they lead to reduced performance or even to failures.
- OHP's show the far better performance, certainly in the evaporator above the condenser mode.
- Only limited evaporator above the condenser mode data is available. For acceleration levels above 1-g (9.8 m/s^2) the extremely scarce data is restricted to the references 15 and 26. This must change because of the different promising applications foreseen in hyper-gravity environments.
- As stated already in the introduction ethanol and water are unattractive working fluids, because of low dp/dT. This is confirmed experimentally (Ref.48).
- Incorporation of one-way (check) valve(s) may improve OHP performance (Ref. 51).
- A hydraulic channel diameter around 2 mm is favoured by most OHP/PHP researchers. It has sense to define this as a kind of a "standard" for future terrestrial research, in order to allow comparison with future and already existing data. For hyper-gravity applications a reduced diameter (around 1 mm) is recommended.

Some remarks can be made on the high acceleration data presented in literature, recalling the high-acceleration experiments done on a 4.5 m diameter centrifuge table with a non-looped acetone (60 % charge) device, consisting of 23 turns of 0.42 m long, 1.1 mm ID, stainless steel capillaries (Ref. 15). The length of the sections was 120 mm for the heating and the adiabatic section, 180 mm for the cooling section. Experiments were done for -90°, 0°, and +90° with respect to tangential. Experimental data confirms that the accelerations influence the pressure drop and the corresponding temperature drop across such devices. For example, while continuously transporting the maximum power 40 W, the finally reached stable heater section temperature increased from 403 K (130 °C) in the 6g thermosyphon mode with the condenser closest to the rotation axis (90°), via 433 K at 0°-g (tangential orientation) and 458 K at 6-g even to 473 K (200 °C) at 12-g in heater closest to the rotation axis mode (-90°). There was no evaporator dry-out for all acceleration conditions specified. The above tests, and vibration tests (frequency 0 to 16 kHz, acceleration 0 to 15 g, amplitude 0 to 7 mm, inclination 0 - 180°) have shown that these oscillating devices are not sensitive for acceleration fields. It is to be noted that the centrifuge table tests properly simulate high-g conditions in aircraft and spinning satellites. But the fluid in lines in radial direction experiences an assisting or counteracting acceleration gradient (as a function of radial position and rotation speed). This gradient is absent in the (super-)gravity environment of planets. The above means that rotation tables are perfectly

adequate to simulate high acceleration level conditions in rotating satellites and manoeuvring aircraft, but they do exactly simulate real planetary gravity only in a very limited case.

TABLE 2. Survey	Type	Fluid	Charg (%)	Inclinat (˚)	Channel mm/mm^2	Turns (Channels	Channel Length	Remarks and Comments
Ref. 41	OHP	ethano	20-80	0 to 90	1.5x1.5	(8)	220 mm	Visualisation study
Ref. 42	OHP	R142b	20-80	30 to 9	1.5x1.5	(20)	220 mm	Many, many useful data
Ref. 43	PHP	ethano R123 water	50	-90 to +90	2 mm ID	(20)	l 10 m in total	Experimental $Q_{max}/Q_0 = 1.8 + 0.06L_e$ $Q_{max}/Q_0 = 2.53 + 0.001h_{lv}$
Ref. 44	OHP	water	30-80	0 to 90	2 mm ID	(up to 150	17.5 /11.15/ 5 m in tot	Experimental $R/R_{max} = 15.775\ N^{-1.1042}$
Ref. 45	OHP	water	40-80	0 main	2 mm ID	(8)	120 mm	Useful: Experimental & Theoretical
Ref. 46	PHP	water?	50	0	unknown	3 (4)	300 mm	Useful: Theoretical only
Ref. 47	??	water	variou	Various Possib	1.5 mm ID	(8)	110 mm	Visualisation study on special structure concept
Ref. 48	OHP	water ethano	10-70	0 & 90	2.2x2.0 1.5x1.0 2 mm ID	12 and 10	104 and 145 mm	Useful: Experimental & Theoretical Conclusion: Need for fluid having higher dp/dT than water and ethanol
Ref. 21	OHP	water ethano R142b soapsu	20-98	0	ID 1.8, 5, 2.4 mm mainly	4 (4)	396 mm	Performance as a function of fill charge, qT and ID was investigated
Ref.22	OHP	water	30-95	90	2.4 mm ID	(20)	290 mm	Performance versus fill charge
Ref.49	OHP	water	50	0?	1 mm ID	4 (4)	150 mm	Theoretical only
Ref.50	OHP	water	..50	0	0.96 ID	8 (8)	430 mm	Performance versus resistance
Ref.15	PHP	acetone	60	-90/0/9	1.1 mm ID	23 (48)	420 mm	Performance in –6 to +12 g
Ref.26	PHP and OHP	acetone water, ethano FC-87	0-50	-90/0/9 -90	1.2x1.2 and 1 mm ID	(48)	100 mm	Performance in –8.4 to +8.4 g of an aluminium PHP. Visualisation study of glass OHP at –90˚ in 1g
Ref.51	OHP	R134a	~50	-90/0/9	2 mm ID	(28)	600 mm	Check valves impact is positive. Further strange, unusual results
Ref.52	PHP	R142b	42	0	2 mm ?	(50)	273 mm	Visualisation study
Ref.53	OHP	R142b	50	0 to 90	1 & 2 mm	1 turn	D: 200, 3 400 mm	Chaos theory predictions: Interesting But strange also
Ref.54	PHP OHP	R142b	20-90	0 to 90	2 mm ID	(16)	400 or 50 mm	Visualisation study: Many, many useful data
Ref.55	OHP PHP	R142b	40-80	60	2 mm ID	3, 4, 5, 6/ 6	?	PHP performs between T-shaped OHP a fully Looped OHP
Ref.56	?	?	?	Any	2.2 mm ID	1500	250 mm	Kenzan, no Heat Lane information
Ref.57	PHP	pentan	?	?	2 mm ID	2	510 total	Visualisation and Modelling
Ref.58	Open	water	?	*)	3.34 ID	2	400 total	*) Heater above condenser.
Ref.59	OHP PHP	water	?	*)	3.34 ID	?	515 total	*) Heater above condenser Theory to be improved

SOME REMARKS ON 1-G SCALING OF PROTOTYPES FOR SUPER-G

NLR's recent modelling and scaling activities (Refs. 12, 40) and the corresponding experimental activities of the last two years (Ref. 26) are straightforward extensions to two-phase loops and oscillating heat transport devices for use in (transient) super-gravity environments (up to 12 g), encountered in spinning spacecraft and during military combat aircraft manoeuvres. Similar activities are reported to be done elsewhere (Refs. 15 to 17).

These extensions led to a reassessment of the applicability and use of thermal-gravitational scaling to graphs like the Figs. 6 and 7. As a general result it was found that that the earlier conclusions dealing with gravity-assist performance (vertical down-flow in some gravity field) remain valid and useable for two-phase loops, including pulsating two-phase loops and other heat transfer devices, in "super-gravity-assist conditions". Though many things will be different in the "anti-gravity" mode, the general thermal-gravitational scaling rules remain valid for "assist and anti" conditions.

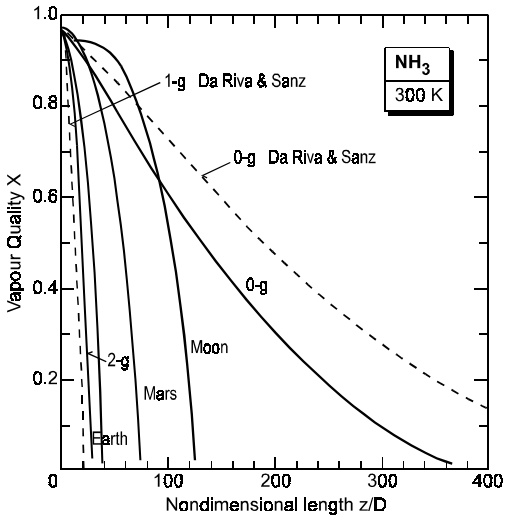

Figure 13. Vapour quality along a reference duct

The above leads to useful quantitative consequences as in the following example of annular condensation of ammonia. Figure 13 presents gravity dependent annular flow condensation curves, calculated using the equations first derived and discussed in the references 60 to 62. These equations are:

$$(dp/dz)t = (dp/dz)_f + (dp/dz)_m + (dp/dz)_g \qquad (14)$$

$$(dp/dz)_f = -(32\dot{m}^2/\pi^2 \rho_v D^5)(0.045/Re_v^{0.2}) * \\ * [X^{1.8}+5.7(\mu_l/\mu_v)^{0.0523}(1-X)^{0.47}X^{1.33}(\rho_v/\rho_l)^{0.261}+ \\ + 8.1(\mu_l/\mu_v)^{0.105}(1-X)^{0.94}X^{0.86}(\rho_v/\rho_l)^{0.52}] \qquad (14a)$$

X is local quality X(z), Reynolds number $Re_v = 4\dot{m}/\pi D\mu_v$ b=2 (laminar), 1.25 (turbulent liquid flow).

$$(dp/dz)_m = -(32\dot{m}^2/\varepsilon^2 \rho_v D^5)(D/2).(dX/dz) * \\ * [2(1-X)(\rho_v/\rho_l)^{2/3} + 2(2X-3+1/X)(\rho_v/\rho_l)^{4/3} + \\ + (2X-1-bX)(\rho_v/\rho_l)^{1/3} + (2b-bX-b/X)(\rho_v/\rho_l)^{5/3} + \\ + 2(1-X-b+bX)(\rho_v/\rho_l)] \qquad (14b)$$

$$(dp/dz)_g = (32\dot{m}^2/\varepsilon^2 \rho_v D^5)\{1-[1+(\rho_v/\rho_l)^{2/3}(1-X)/X]^{-1}\} * \\ * [\varepsilon^2 D^5 g \cos\nu(\rho_l-\rho_v)\rho_v/32\dot{m}^2] \qquad (14c)$$

$$(1-\alpha)/\alpha = S(\rho_v/\rho_l)X/(1-X) \qquad (15)$$

$$S = (\rho_l/\rho_v)^{1/3} \qquad (16)$$

$$\dot{m}\, h_{lv}(dX/dz) = -h\pi D[T(z)-T_s] \qquad (17)$$

$$h = 0.018(\theta\rho_l^{1/2}/\mu_l)Pr_l^{0.65}|-(dp/dz)_t|^{1/2}D^{1/2} + R(4\lambda_l/D) * \\ * \ln[1+(\rho_v/\rho_l)^{2/3}(1-X)/X] \quad 0 < R < 1. \qquad (18)$$

$$\Delta p_t = \int_0^{L_c} (dp/dz)_t.dz\,. \qquad (19)$$

$$F(dX/dz, X) = 0. \qquad (20)$$

Consequently, for say 10-g the above equations predict a 10-g full condensation length of the order of 10 D, as it also can be derived (by extrapolation) from the curves in the figure.

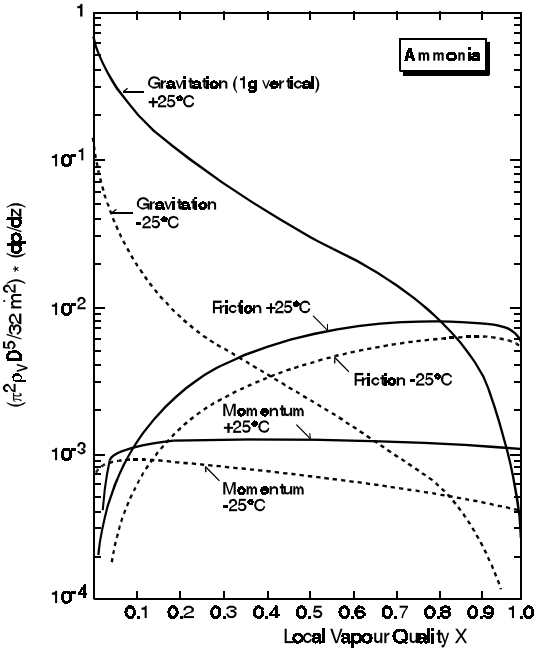

Figure 14. Pressure drop constituents at –25 and +25 °C

Fig. 14 depicts the vapour quality dependence of the pressure gradient constituents (friction, momentum and gravity) in two-phase annular flow, calculated according to the aforementioned equations, for ammonia at +25°C and -25°C. The resulting total pressure gradient prediction for the TPX configuration was confirmed by the data gathered during the Space Shuttle flight STS60 in February 1994 (Ref. 63).

That the consequences for the scaling of a super-gravity prototype system by a 1-g model follow from the Figs. 6 and 7, is illustrated by the following example. For an ammonia prototype system P, intended for operation around 320 K in a 10-g environment, Fig. 6 reads a value (10g x Mo_P) of about $1.5\ 10^{13}$. Since g is about 10 m/s^2. As proper scaling requires that the Morton number in prototype and model are to be identical, the ordinate for the 1-g model becomes $10x1.5x10^{11} = 1.5x10^{12}$. The latter value corresponds to acetone at say 310 K. As for proper scaling Eö = (We/Fr) in prototype and model are to be the same, one obtains the relation $(D_M/D_P)^2 = (g_P/g_M)(\sigma/\rho_l)_P/(\sigma/\rho_l)_M$. Fig. 7 yields the geometric scaling factor by inserting the g-ratio (10) and the ordinate values corresponding to ammonia at 320 K (0.0055) and acetone at 35°C

(0.0053). The result is a geometric scaling factor d_M/d_P around 3.2, maybe too large for novel pulsating/oscillating devices (as these have to fulfill an additional capillary criterion, as it was elucidated earlier in this report), but not unrealistic or impossible for two-phase loops. Similar considerations for water (at 310 K) as the model fluid yield a d_M/d_P somewhat less than 2, ideal for scaling two-phase systems, both loops and pulsating/oscillating ones.

But as said: many things will be different in "assist and anti" conditions. This is clearly illustrated by Fig. 14, if one looks at the fact that at +25°C gravity overrules the other pressure constituents, hence is the driving mechanism, for quality values up to approximately 0.7. The curve for 10 g is simply obtained by shifting the gravity curve one decade upwards, which means that gravity is overwhelming the other constituents up to a quality of 0.97 (where the flow pattern is homogeneous). When the direction of gravity is reversed, the situation is clearly different. Gravity will act against the other constituents, meaning fall back of the liquid, which initially leads to a steep increase of the saturation temperature to deliver the vapour pressure needed to maintain transport (of course not in the annular flow pattern anymore, but in the churn or slug/plug flow regime), but soon stopping the flow in the above mentioned quality ranges.

A complicating factor is the fact that the pressure drops substantially increase, and the equations, derived for nearly isothermal conditions (hence constant fluid properties), no longer hold and have to be replaced by far more complicated ones. The latter is also valid for pulsating/oscillating devices, which essentially need, to operate, relatively large temperature differences between evaporator and condenser.

A SIMPLE QUANTITATIVE MODEL DEFINING THE FUTURE TESTING APPROACH

The relevant published results of experiments were used to establish a simple quantitative model for oscillating (pulsating) heat transfer devices. The way that was done (Refs. 12, 40) is described hereafter.

A first step in a logic approach to develop pulsating two-phase test devices is to dimension these such that test outcomes can be compared directly to the performance data of the described synchronised oscillating single-phase device.
A second step is to assume that the single-phase device (Fig. 10) consists of 85 identical cylindrical channels with an average internal diameter d = 1 mm. This represents the actual configuration of 31 glass capillaries (1 mm ID) and 54 triangular channels present between these capillaries, thus yielding the total liquid cross-sectional area $A_l = 85*\pi/4 \approx 67$ mm^2. For simplicity reasons the tube length is assumed to be equal to the displacement length: $L = \Delta z = 125$ mm. The power transported by each capillary can be calculated from the data presented. For the maximum transport case, being for frequency f = 8 Hz and temperature difference $\Delta T = 56$ K, this becomes $(\pi/4)\, d^2\, 2.9\, 10^6 = (\pi/4)\, 10^{-6} \approx 2.3$ W.

The third step is the simplification to consider the pulsating two-phase device (Fig. 5) to be, in essence, a configuration of identical, parallel elements, each one transporting the same amount of power, driven by the vapour pressure difference between the heat input (evaporator) section and the cooling (condenser) section. In addition, the working fluid and dimensioning of the two-phase and single-phase devices are identical: The working fluid is water, the capillary diameter d = 1 mm, the evaporator and condenser length are $L_e = L_c = L =$ 125 mm. In the first approximation, it is assumed that there is no adiabatic section. The main differences between the two devices pertain to the driving mechanisms, the heat transfer processes and the heat transfer locations.

A mechanical actuator is the driver of the oscillating axial movement of the liquid in the single-phase device. Only specific heat is exchanged over the entire capillary tube length L in two sequential radial (conduction) steps. In the first half of the period, heat is transferred in radial direction from the hot fluid in the core to the thin Stokes layer (and the tube wall). In the second half of the period, the heat is moved back to the cold fluid in the core.

In the two-phase device heat is simultaneously exchanged in radial direction, mainly by conduction, plus some convection, at two different locations. The heat is fed via the wall to the working fluid in the hot input (evaporator) section. The heat is extracted from the fluid via the wall in the cold section (condenser). This heat transfer, via the specific heat of the liquid, looks more or less identical in the two systems. The transfer difference (i.e. two-step sequential at one location, respectively simultaneous heat addition and extraction at two different locations) suggests that it is reasonable to assume that the transported power in the two-phase case is, for $\Delta T =$ 56 K, twice the value for a single-phase capillary (4.6 W). Alternatively, it can also be assumed that $\Delta T = 28$ K only, at a power transport of 2.3 W.

However, there is an additional latent heat transfer contribution in the two-phase device: The heat transported via the vapour bubble that grows in the heat input section (evaporator) by evaporation of a liquid micro-layer (Ref. 38). This bubble collapses in the condenser, releasing its latent heat. The pressure

difference, between the (super-heated) vapour in the evaporator and the saturated vapour in the condenser, is the driving force moving the hot liquid slug from evaporator to condenser, plus moving at the same moment a similar cold slug from condenser back to the same or a neighbouring evaporator. The power transported by latent heat can be obtained by calculating the energy needed to create 8 bubbles, of length L and diameter d, per second. Consequently one obtains 8 $(\pi/4)d^2L\rho_v h_{lv} = 8(\pi/4).10^{-6}$-(1/8) (0.2) $(2.25* 10^6 \approx 0.45$ W, which constitutes a minor, but non-negligible contribution.

The pressure head across the capillary single-phase water system can be calculated as follows. The displacement of 125 mm at frequency 8 Hz yields a liquid velocity v = 2 m/s. For water around 300 K, the Reynolds number Re_l is around 2000, which means laminar flow. Consequently, the required pressure drop is 8 kPa, according to the equation

$$\Delta p = 4 * (16 / Re_l) (L / d) (\rho_l v^2 / 2). \quad (21)$$

In the corresponding two-phase device the required pressure difference has to be far larger, because of several reasons. In the first place twice the single-phase device mass (a hot and a cold slug) has to be moved. Secondly, this double mass has to be forced through a 180 degrees bend instead a straight channel. Further, the length of the adiabatic section (L_a) is of course, in reality, never equal to zero. Finally, the process concerns all except fully developed flow, hence there is a liquid acceleration term to be added.

To get a feeling for the magnitude of these pressure enlarging effects, the length L_a is taken to be also 125 mm (L_a = L), as an example. This has impact on the contribution of the power transport via the latent heat of evaporation. This contribution will be around 0.9 W, since the length of each of the 8 vapour bubbles, being generated and collapsing in one second, is L_a + L (hence 2L, instead L). The average liquid velocity becomes v = 4 m/s. For water around 300 K, the Reynolds number Re_l now lies around 4000, which means turbulent flow. Consequently the required pressure drop has to be calculated according to

$$\Delta p = 4\ (0.0791)\ Re^{-¼}\ (L / d)\ (\rho_l v^2 / 2). \quad (22)$$

As discussed in textbooks (e.g. Ref. 64), the effect of the two bends can be accounted for by adding an extra length of 50 D. The pressure drop can now be calculated, according to equation (22), by inserting the different parameter values and by replacing L by 2 (2L + 50 d). The result is 480 kPa. To be complete an inertia term, accounting for the acceleration of the slugs eight times per second, has to be added: 8 ($\rho_l v^2$ / 2), hence 16 kPa, yielding about 500 kPa for the pressure difference required. Consequently, it can be concluded from the water curve in figure 1, that the two-phase device has to operate at a hot section temperature of at least 350 K (80 °C), to be able to deliver the pressure drop required. Figure 1 makes also clear that more or less comparable power can be transported by ammonia, R12, acetone, etc. Though at comparable ΔT's, this will be realised at far lower operating temperatures, as these fluids show a steeper dp/dT-relation.

The results of the above simple approach and of the detailed modelling of the physical processes, including mass-spring simulations, currently is compared and will be compared in the near future to experimental data, resulting from further experimenting at NLR. The experimental activities include many high-acceleration experiments on a rotation table. The experiments have been, are, and will be carried out both with all-metal devices, and with all-glass devices (Ref. 26). Additional experiments will be executed using a helical (spring-like) configuration of transparent (PTFE or polyethylene) flexible tubing, equipped with a simple one-way valve in order to influence direction and frequency of the periodic behaviour of a closed-loop configuration. Experiments pertain to various working fluids and different locations of hot and cold sections, to different lengths of adiabatic section, to various orientations, and to different acceleration levels in various directions.

VERSATILE TEST RIG & TEST SET-UP

A versatile rig for experimenting with different pulsating/oscillating HTD's was designed and built. The rig is shown in the drawing (Fig. 15) and the photograph (Fig. 16). Fig. 17 depicts the experimental set-up. The test section of the rig (left) consists of a steel frame, which can be rotated with respect to the steel support (right) to allow the investigation of tilt on the HTD performance. The inclination can be arbitrarily adjusted within the range between the + 90 degrees full thermosyphon mode (condenser vertical above evaporator) and the –90 degrees full anti-gravity mode (evaporator on top, vertical above condenser). Both the evaporator section and the condenser section are as good as possible thermally isolated: from the steel frame by spacers of insulating materials, to minimise the thermal leak path through the frame, from the environment by covers of polystyrene. The evaporator section is heated by an electric heater element. Input voltage (V) and current (I) will be measured. The condenser section is liquid cooled. The coolant flow rate (ű) is measured. The temperature difference between coolant at the outlet and at the inlet is measured also.

The basic test item is a closed end HTD, a Pulsating Heat Pipe (PHP), consisting of 180 degrees bent stainless steel tubes (OD 3 mm, ID 2 mm) in the condenser and evaporator sections, connected by flexible transparent PTFE tubing (OD 3 mm, ID 2 mm). The length of the latter (162 mm) tubing can be

increased to study the influence of length on the PHP performance. Currently this implies non-straight transparent sections, which is not ideal for flow visualisation. This problem can be solved easily by cutting the frame in two halves, which can be bolted to steel.(connecting) interface parts at both sides. The latter parts are rotatable with respect to the steel support. Each one must have several holes (or one long elliptic hole) to realise mounting of the frame halves in different ways, in order to meet longer PHP dimensions. In this way it can be guaranteed that the transparent sections are always straight. The rig is equipped with various thermocouples measuring the temperatures at crucial locations and a pressure sensor at the filling valve to study the history of internal PHP. A second pressure gauge is at the draining valve.

Parameters, which can be varied, are the already mentioned inclination with respect to gravity, input power, the coolant flow rate (to obtain a balance between isothermality and a measurable qpT), plus the filling ratio.

In order to change from PHP configuration to the looped Oscillating Heat Pipe (OHP) configuration in a later phase of the experimental programme, the filling tube and the draining tube are to be connected by a tube. This can be easily realised by adding T-pieces at the filling and draining lines. By installing a valve in this line, one can simply change switch between the OHP and PHP options. The including of one-way valves, to study their impact on the performance, is even simpler: They can be inserted almost everywhere in the transparent tubing.

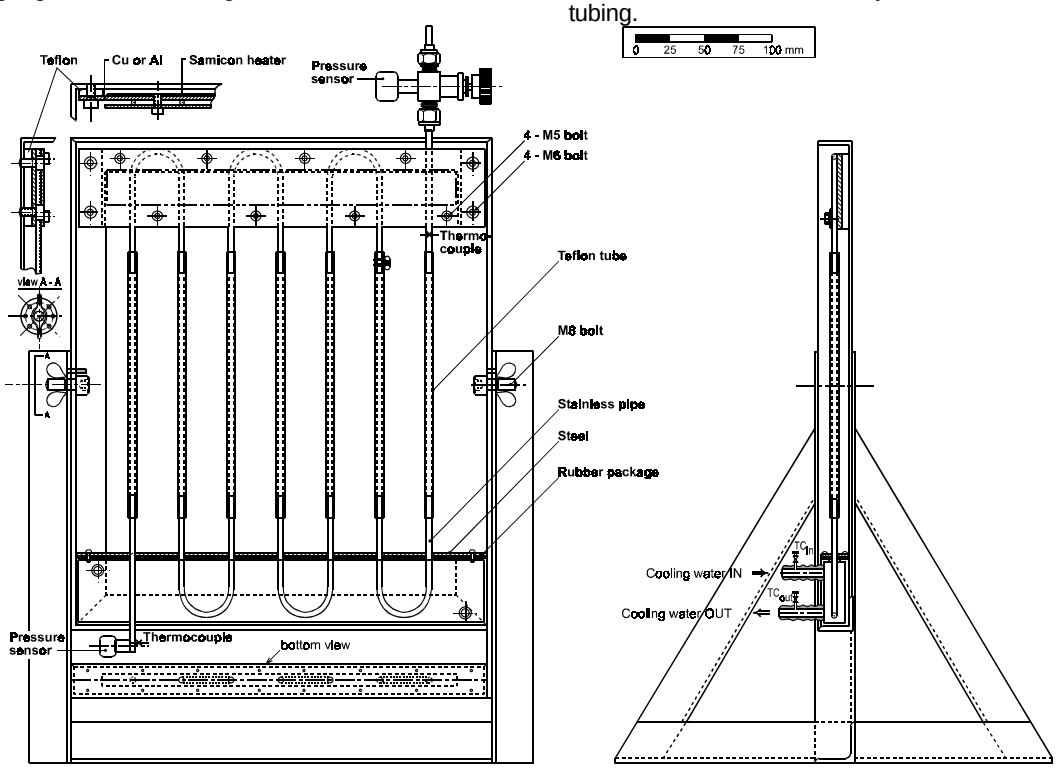

Figure 15. Versatile rig for experimenting with looped oscillating and closed end pulsating HTD's

Adjusted parameters for the experimental set-up. are inclination, length of the test item, filling ratio. Further are to be measured, registered, stored and manipulated (using the data acquisition system and the PC):

- The voltage V and heater current I, yielding the electric input power Q_{el}.
- The coolant temperature difference qpT and flow rate ű, yielding the power output since the density ɟ$_l$ and specific heat Cp_l of the coolant are known.
- Many temperatures, by various thermocouples and the IR camera.
- Pulsating frequencies by the high-speed video visualisation (a stroboscope can be used as light source) and thermal visualisation (IR pictures)

Sound detection and bubble velocity measurement preferably has to be installed. For the sound detection one can for instance use the PC and an electret microphone element. Digital recording can be simply done using standard Windows software. The analysis

(FFT) can be done with sound manipulation. Powering a two-wire electret capsule from the soundcard bias voltage output can be done e.g. by a circuit shown at http://www.hut.fi/Misc/Electronics/circuits/microphone_powering.html.

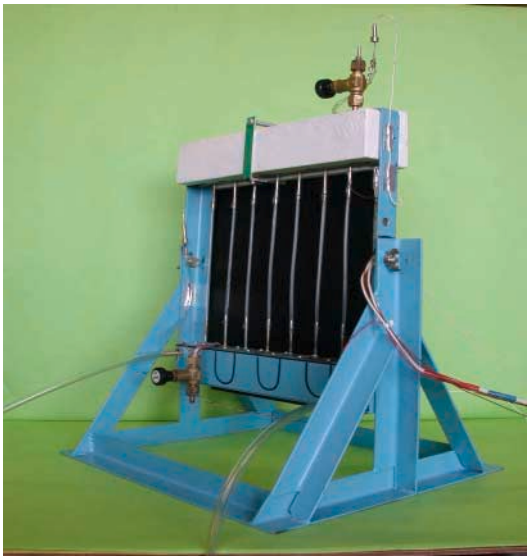

Figure 16. Picture of the versatile test rig

This particular circuit is suitable for interfacing two wire electret microphone capsules to soundcards (Sound Blaster soundcards), which supply bias voltage for powering the electret microphones. Detailed information on electret microphones is published at http://www.jielectronics.com/microphone_specs.html and at http://www.flourish.com.hk/2eh-electret.htm). Optical liquid/bubble velocity detection can be done with 4 light slits (LED-photodiode), using a reasonably fast data acquisition system.
By running the test with an empty test item (PHP or OHP), the losses by radiation and by conduction via the heat leak path through the steel frame can be calibrated as a function of the hot boundary temperature (for a fixed sink or coolant temperature). These losses are to be subtracted from the input power Q_{el} to determine the power transported by the test item itself.

CONCLUDING REMARKS

In conclusion, it is remarked that the presented information summarises the approach for the thermal-gravitational scaling of two-phase systems in general. Results of similarity considerations are given. Modelling results are discussed, including comparison with experimental data. The discussions include gravity-assist system aspects and issues of operation against gravity or super-gravity. They pertain to capillary pumped and mechanically pumped two-phase loops, pulsating two-phase loops, and all other single-phase and two-phase oscillating (pulsating) devices. A simple rationale to get a (quantitative) feeling for the development of pulsating devices for useful experiments is given.

In addition two very critical issues are to be stressed (again and again), since they are not adequately discussed in literature (most probably because one did not recognise these). First, planetary super-gravity has a constant magnitude felt in each part of any (two-phase heat transfer) device. This principally differs from the “super-g” accelerations in spinning satellites, in military combat aircraft and on turntables. In the latter, the g-vectors have gradients across a device. Those gradients depend on local position and orientation with respect to the rotation axis. Second, in pulsating (pressure driven) two-phase loops heat transfer is by the latent evaporation/condensation heat. This means that the working fluid selection will be based on high latent heat, in addition to high a dp/dT to deliver a minimum temperature drop driving force for the system. The other pulsating two-phase devices also require a fluid with a high dp/dT. But as it was shown that in the latter devices the majority is by caloric (specific) heat of the liquid, it is clear that a high specific heat, high dp/dT fluid will be preferred. The question is even to be raised whether there exists an ideal high specific heat, high dp/dT fluid, having also a low latent heat. This because low latent heat means that, as the driving bubble growth is fast, the pulsation frequency and heat transport efficiency will increase. If such a fluid does not exist, there has certainly to be looked at a fluid with an optimum combination of the above properties.

It is also remarked that for planetary reduced and super-g conditions there is no information at all on flow pattern maps and the boundaries between the different flow regimes. Therefore, and as it is also expected that the various items will substantially differ from the (hardly available) existing 1-g ones, the creation of flow pattern maps for super-gravity environment has been started at NLR. Fortunately, investigators in the US recently started to follow the NLR approach in this respect (Ref. 65).

The discussions focus on, in addition to “classical” two-phase loops, also pulsating loops and other novel oscillating/ pulsating heat transfer devices. A review of their most relevant recent publications (also on high acceleration issues) is given. The baseline for comparing the experimental data in these and in future publications on these devices, a single-phase heat transfer device, is elucidated.

A simple quantitative model to define future testing of oscillating/pulsating heat transfer devices is presented. Based on this and the literature review, a versatile test rig has been designed and built. The rig and the test set-up are described. The test programme and the filling procedure are given in Ref. 66.

ACKNOWLEDGMENTS

This is to acknowledge the many fruitful discussions with the ISAS host Professor Dr. Y. Kobayashi, and the excellent support of his collaborators Messrs Sato, who built the test rig and test set-up, and Ogawa, who solved all PC related (HW and SW) problems.

REFERENCES

1. Delil, A.A.M., Two-Phase Heat Transport Systems for Spacecraft – Scaling with Respect to Gravity, NLR-TP-89127, SAE 891467, 19th Int. Conf. on Environmental Systems, San Diego, USA, 1989, SAE Trans. J. Aerospace, **98**, 1989, 554-564.
2. Delil, A.A.M., Thermal Gravitational Modelling and Scaling of Two-Phase Heat Transport Systems: Similarity Considerations and Useful Equations, Predictions versus Experimental Results, NLR-TP-91477, Proc. 1st European Symp. Fluids in Space, Ajaccio, France, 1991, ESA SP-353, 579-599.
3. Delil, A.A.M., Two-Phase Heat Transport Systems for Space: Thermal Gravitational Modelling and Scaling Predictions Versus Results of Experiments, Proc. ASME-JSME Forum on Microgravity Fluid Flow, Portland, USA, 1991, ASME-FED- 111, 21-27.
4. Delil, A.A.M., Thermal Scaling of Two-Phase Heat Transport Systems for Space: Predictions versus Results of Experiments, NLR-TP-91477, Proc. 1991 IUTAM Symp on Microgravity Fluid Mechanics, Bremen, Germany, 469-478.
5. Delil, A.A.M., On Thermal-Gravitational Modelling, Scaling and Flow Pattern Mapping Issues of Two-Phase Heat Transport Systems, NLR-TP-98268, SAE 981692, 28th International Conference on Environmental Systems, Danvers, USA, 1998, SAE Trans. J. Aerospace, **107**, 1998.
6. Delil, A.A.M., Aerospace Heat and Mass Transfer Research for Spacecraft Thermal Control Systems Development, NLR-TP-98170, Heat Transfer 1998, Proc. 11th Int. Heat Transfer Conference, Kyongju, Korea, 1998, 1, Keynotes, 239-260.
7. Delil, A.A.M., Unsolved Aerospace Heat and Mass Transfer Research Issues for the Development of Two-Phase Thermal Control Systems for Space, Proc. Int. Workshop Non-Compression Refrigeration & Cooling, Odessa, Ukraine, 1999, 21-42.
8. Delil, A.A.M., Thermal-Gravitational Modelling, Scaling and Flow Pattern Mapping Issues of Two-Phase Heat Transport Systems, Conference on Applications of Thermophysics in Microgravity and Breakthrough Propulsion Physics, AIP Conf. Proc. 458, Space Technology & Applications International Forum, Albuquerque, NM, USA, 1999, 761-771.
9. Delil, A.A.M., Some Critical Issues in Developing Two-Phase Thermal Control Systems for Space, NLR-TP-99354, Proc. 11th Int. Heat Pipe Conference, Tokyo, Japan, 1999, Vol.3, Keynote and Invited Lectures, 61-79.
10. Delil, A.A.M., Microgravity Two-Phase Flow and Heat Transfer, NLR-TP-99429, Chapter 9 of Fluid Physics in Microgravity, (Monti, R., Ed.), Overseas Publishing Associates, Reading UK, 2001.
11. Delil, A.A.M., Extension of Thermal-Gravitational Modeling & Scaling of Two-Phase Heat Transport Systems to Super-Gravity Levels and Oscillating Heat Transfer Devices, Keynote Lecture, 6th Int. Heat Pipe Symposium, Chiang Mai, Thailand, 2000, Pre-Prints, 15-32, and ESA Proc. Two-Phase 2000 Workshop, Noordwijk, Netherlands, 2000.
12. Delil, A.A.M., Thermal-Gravitational Modelling and Scaling of Heat Transport Systems for Applications in Different Gravity Environments: Super-Gravity Levels & Oscillating Heat Transfer Devices", NLR-TP-2000-213, SAE-2000-01-2377, Proc.30th International Conference on Environmental Systems & 7th European Symposium on Space Environmental Control Systems, Toulouse, France, 2000.
13. Delil, A.A.M., Fundamentals of Gravity Level Dependent Two-Phase Flow and Heat Transfer – A Tutorial, and Thermal-Gravitational Modelling, AIP Conf. Proc., Space Technology & Applications International Forum, Albuquerque, USA, 2001, 209-220.
14. Delil, A.A.M., Scaling of Two-Phase Heat Transport Systems from Micro-Gravity to Super-Gravity Levels, AIP Conf. Proc., Space Technology & Applications International Forum, Albuquerque, USA, 2001, 221-229.
15. Kiseev, V.M., Zolkin, K.A., The Influence of Acceleration on the Performance of Oscillating Heat Pipe, Proc. 11th Int. Heat Pipe Conference, Tokyo, Japan, 1999, Vol.2, 154-158.
16. Romestant, C., Sophy, T., Alexandre, A., Dynamic of heat pipe behavior under cyclic body forces environment, Proc. 11th Int. Heat Pipe Conference, Tokyo, Japan, 1999, **2**, 1-6.
17. Ku, J., et al., Transient Behaviors of a Miniature LHP Subjected to Periodic Accelerations Parallel to the Axis of Evaporator and Hydro-accumulator, Proc.30th International Conference on Environmental Systems & 7th European Symposium on Space Environmental Control Systems, Toulouse, France, 2000.
18. Tamburini, P., "T-System", Proposal of a New Concept Heat Transport System, Proc. 3rd International Heat Pipe Conference, Palo Alto, USA, 1978, AIAA CP-784, 346-353.
19. Lund, K.O., Baker, K.W., Weislogel, M.M., The Vapor-Pressure Pumped Loop Concept for Space Systems Heat Transport, Proc. 1st International. Conference on Aerospace Heat Exchanger Technology 1993, Palo Alto, USA, (Shah, R.K., Hashemi, A.), Elsevier, Amsterdam 1993, 45-55.
20. Borodkin, A.A., Kotlyarov, E.Yu, Serov, G.P., Evaporation-Condensation Pump for Providing of Working Fluid Circulation in Two-Phase Heat Transferring System, SAE 951508, 25th International Conference on Environmental Systems, San Diego, CA, USA, 1995.
21. Nishio, S., Oscillatory-Flow Heat Transport Device, Proc. 11th International Heat Pipe Conference, Tokyo, Japan, 1999, Pre-prints, Vol.3, Keynote and Invited Lectures, 39-49.
22. Hosoda, M., Nishio, S., Shirakashi, R., Meandering Closed-Loop Heat-Transport Tube (Propagation Phenomena of Vapor Plug), Proc. 5th ASME-JSME Thermal Engineering Conference, San Diego, CA, USA, 1999, 1-8.

23. Nishio, S., Shin, H-T, Oh, S-J., Oscillation-Controlled Heat-Transport Tubes (Effect of Transition from Laminar to Turbulent Flow on Effective Conductivity), Heat Transfer 1998, 11th International Heat Transfer Conference, Kyongju, Korea, 1998, Vol. 3, 317-322.
24. Wong, T.N., et al., Theoretical Modelling of Pulsating Heat Pipe, 11th International Heat Pipe Conference, Tokyo, Japan, 1999, Pre-prints, Vol.2, 159-163.
25. Akachi, H., Motoya, S., Maezawa, S., Thermal performance of capillary tunnel type flat heat pipe, Proc. 9th International Heat Pipe Conference, Albuquerque, NM, USA, 1995, LA-UR-97-1500, 1997, Vol. 1, 88-96.
26. Es, J. van, Woering, A.A., High-Acceleration Performance of the Flat Swinging Heat Pipe, Proc.30th International Conference on Environmental Systems & 7th European Symposium on Space Environmental Control Systems, Toulouse, France, 2000.
27. Terpstra, M., Veen, J.G. van, Heat Pipes: Construction and Applications, EUR 10925 EN, Elsevier, London, 1987.
28. Maezawa, S., et al., Thermal Performance of Capillary Tube Thermosyphon, Proc. 9th International Heat Pipe Conference, Albuquerque, NM, USA, 1995, LA-UR-97-1500, 1997, Vol. 21, 791-795.
29. Smirnov, H.F., Kuznetsov, I.O., Borisov, V.V., Approximate Pulsating Heat pipe Theory and Experiment, Proc. Int. Workshop Non-Compression Refrigeration & Cooling, Odessa, Ukraine, 1999, 121-125.
30. Wallis, G.B., One-dimensional Two-phase Flow, McGraw-Hill, New York, 1969.
31. Murphy, G., Similitude in Engineering, Ronald Press, New York, USA, 1950.
32. Bretherton, F.P., The Motion of Long Bubbles in Tubes, J. of Fluid Mechanics, **10**, 1961, 161-188.
33. Hattori, S., Rept. Res. Inst. Tokyo Imp. Univ., **115**, 1935.
34. Kurzweg, U.H., Zhao, L., Heat Transfer by High-frequency Oscillations: A New Hydrodynamic Technique for Achieving Large Effective Conductivities, Physics of Fluids, **27,** 1984, 2624-2627.
35. Kurzweg, U.H., Enhanced Heat Conduction in Fluids Subjected to Sinusoidal Oscillations, Trans. ASME, J. Heat Transfer**, 107,** 1985, 459**-**462.
36. Kurzweg, U.H., Lindgren, E.B., Lothrop, B., Onset of Turbulence in Oscillatory Flow at Low Womersley Number, Physics of Fluids A, **1** (12), 1989, 1972-1975.
37. Watson, E.J., Diffusion in Oscillatory Pipe Flow, J. Fluid Mech., **133**, 1983, 233-244.
38. Inada, T., Tahara, M., Saitoh, K-I., Longitudinal Heat Transfer in Oscillatory Flows in Pipe Bundles of Various Cross Sections, JSME International Journal, Series B, 43, No. 3, 2000, 460-467.
39. Inada, T., Kubo, T., Enhanced Heat Transfer through Oscillatory Flow, Heat Transfer – Japanese Research, **22**, 5, 1993, 480-492.
40. Delil, A.A.M., Modelling and Scaling of Oscillating or Pulsating Heat Transfer Devices Subjected to Earth Gravity and to High Acceleration Levels, AIP Conf. Proc., Space Technology & Applications International Forum, Albuquerque, USA, 2001, 230-240.
41. Lee, W.H., et al., Flow Visualization of Oscillating Capillary Tube Heat Pipe, 11th Int. Heat Pipe Conference, Tokyo, Japan, 1999, Pre-prints, Vol.2, 149-153.
42. Lee, W.H., et al., Characteristics of Pressure Oscillations in Self-excited Oscillating Heat Pipe Based on Experimental Study, 6th Int. Heat Pipe Symposium, Chiang Mai, Thailand, 2000, preprints 263-272.
43. Rittidech, S., et al., Effect of Inclination Angles, Evaporator Section Lengths and Working Fluid Properties on Heat Transfer Characteristics of Closed-End Oscillating Heat Pipe, 6th Int. Heat Pipe Symposium, Chiang Mai, Thailand, 2000, Pre-prints 281-288.
44. Charoensawan, P., et al., Effect of Inclination Angles, Filling Ratios and Total Section Lengths on Heat Transfer Characteristics of Closed-Loop Oscillating Heat Pipe, 6th Int. Heat Pipe Symposium, Chiang Mai, Thailand, 2000, Pre-prints 289-298.
45. Zuo, Z.J., North, M.T., Miniature High Heat Flux Heat Pipes for Cooling of Electronics, SEE 2000, Hong Kong, China, 2000.
46. Wong, T.N., Theoretical Modelling of Pulsating Heat Pipe**,** 11th Int. Heat Pipe Conference, Tokyo, Japan, 1999, Pre-prints, Vol.2, 159-163.
47. Schneider, M, Yoshida, M., Groll, M., Investigation of Interconnected Mini Heat Pipe Arrays for Micro Electronics Cooling, 11th Int. Heat Pipe Conference, Tokyo, Japan, 1999, Pre-prints, Vol.1, 1-6.
48. Schneider, M, et al., Visualization of Thermofluiddynamic Phenomena in Flat Plate Closed Loop Pulsating Heat Pipes, 6th Int. Heat Pipe Symposium, Chiang Mai, Thailand, 2000, Pre-prints 235-247.
49. Buz, V.N., The Modeling of Non-Stationary Phenomena in Two-Phase Heat Transferring Devices, Proc. Int. Workshop Non-Compression Refrigeration & Cooling, Odessa, Ukraine, 1999, 106-111.
50. Smirnov, H.F., Kuznetsov, I.O., Borisov, V.V., The Modeling of Non-Stationary Phenomena in Two-Phase Heat Transferring Devices, Proc. Int. Workshop Non-Compression Refrigeration & Cooling, Odessa, Ukraine, 1999, 121-125.
51. Miyazaki, Y., Polasek, F., Akachi, H., Oscillating Heat Pipe with Check Valves, 6th Int. Heat Pipe Symposium, Chiang Mai, Thailand, 2000, Pre-prints 257-261.
52. Miyazaki, Y., Arikawa, M., Oscillatory Flow in Oscillating Heat Pipe, 11th Int. Heat Pipe Conference, Tokyo, Japan, 1999, Pre-prints, Vol.2, 143-148.
53. Maezawa, S., Sato, F., Gi, K., Chaotic Dynamics of Looped Oscillating Heat Pipes (Theoretical Analysis on Single Loop), 6th Int. Heat Pipe Symposium, Chiang Mai, Thailand, 2000, Pre-prints 273-280.
54. Gi, K., Sato, F., Maezawa, S., Flow Visualization Experiment on Oscillating Heat Pipes, Flow Visualization Experiment on Oscillating Heat Pipes, 11th Int. Heat Pipe Conference, Tokyo, Japan, 1999, Pre-prints, Vol.2, 149-153.
55. Gi, K, Maezawa, S., CPU Cooling of Notebook PC by Oscillating Heat Pipe, 11th Int. Heat Pipe Conference, Tokyo, Japan, 1999, Pre-prints, Vol.2, 166- 169.
56. Rossi, L., Polasek, F., Thermal Control of Electronic Equipment by Heat Pipes and Two-Phase Thermosyphons, 11th Int. Heat Pipe Conference, Tokyo, Japan, 1999, Pre-prints, Vol.3, handout.
57. Swanepoel, G., Taylor, A.B., Dobson, R.T., Theoretical Modeling of Pulsating Heat Pipes, , 6th Int. Heat Pipe Symposium, Chiang Mai, Thailand, 2000, Pre-prints, 227-234.

58. Dobson, R.T., Modeling of an Open Oscillatory Heat Pipe, 6th Int. Heat Pipe Symposium, Chiang Mai, Thailand, 2000, Pre-prints 249-256.
59. Dobson, R.T., Harms, T.M., Lumped Parameter Analysis of Closed and Open Oscillatory Heat Pipe, 11th Int. Heat Pipe Conference, Tokyo, Japan, 1999, Pre-print **2**, 137-142.
60. Soliman, M. & Schuster, J.R., Berenson, P.J., A General Heat Transfer Correlation for Annular Flow Condensation, Trans. ASME C, J. Heat transfer, 1968, **90,** 267-276.
61. Delil, A.A.M., Gravity Dependence of Pressure Drop and Heat Transfer in Straight Two-Phase Heat Transport System Condenser Ducts, NLR-TP-92167, SAE 921168, 22nd Int. Conf. on Environmental Systems", Seattle, USA, 1992, SAE Trans., J. of Aerospace, **101**, 1992, 512-522.
62. Delil, A.A.M., Gravity Dependent Condensation Pressure Drop and Heat Transfer in Ammonia Two-Phase Heat Transport Systems, NLR-TP-92121, AIAA 92-4057, National Heat Transfer Conf., San Diego, USA, 1992.
63. Delil, A.A.M. et al., TPX for In-Orbit Demonstration of Two-Phase Heat Transport Technology - Evaluation of Flight & Post-flight Experiment Results, NLR-TP-95192, SAE 95150, 25th Int. Conf. on Environmental Systems, San Diego, USA, 1995.
64. Incroprera, F.P., De Witt, D.P., Fundamentals of Heat and Mass Transfer, John Wiley, New York, 1990.
65. Miller-Hurlbert, K., Flow Dynamics for Two-Phase Flow in Partial Gravities, Ph.D. Thesis, Univ. of Houston, 2000.
66. Delil, A.A.M, Pulsating & Oscillating Heat Transfer Devices in Acceleration Environments Ranging from Micro-Gravity to Super-Gravity, A review of research results presented in literature, Assessment of commonalities & differences, A baseline to compare experimental data, Development of a versatile test set-up, and Experiment programme definition, NLT-CR-2001-299, 2001.

NOMENCLATURE

A	area ($m^{2)}$
Ar	Archimedes number = $Mo^{½}$ (-)
B	proportionality factor (-)
Bo	Bond number = $g D^2 \rho_l /4\sigma$ (-)
Boil	boiling number = $\Delta H/h_{lv}$ = Boil (-)
C	conductance (W/K)
Cp	specific heat at constant pressure (J/kg.K)
D	diameter (m)
d	diameter of capillary or of curvature (m)
E	enhancement factor (-)
Eö	Eötvös number = $g D^2 \rho_l /\sigma$ (-)
Eu	Euler number = $\Delta p/\rho v^2$ (-)
f	frequency (Hz)
Fr	Froude number = v^2/gD (-)
g	gravitational acceleration (m/s^2)
H	enthalpy (J/kg)
h	heat transfer coefficient ($W/m^2.K$)
h_{lv}	latent heat of vaporisation (J/kg)
I	current (A)
j_l	superficial liquid velocity = $v_l (A_l /A_t)$ (m/s)
j_v	superficial vapour velocity = $v_v (A_v /A_t)$ (m/s)
k	thermal conductivity (W/m.K)
L	length (m)
Ma	Mach number = $v/(\partial p/\partial \rho)_s^{1/2}$ (-)
Mo	Morton number = $\rho_l \sigma^3/\mu_l^4$ g (-)
Mu	Inverse viscosity number ≈ $\mu_l(gD^3 \rho_l^2)^{-1/2}$(-)
$\dot{m}$	mass flow rate (kg/s)
N	number of turns (-)
Nu	Nusselt number = hD/λ (-)
p	pressure (Pa = N/m^2)
Pr	Prandtl number = μCp/λ (-)
Q	power (W)
Q	heat flux (W/m^2)
Re	Reynolds number = ρvD/μ (-)
S	slip factor, ratio of velocities of phases (-)
T	temperature (K = 273 + °C)
t	time (s)
v	velocity (m/s)
v*	dimensionless velocity = $v / (g D)^{½}$ (-)
v	velocity (m/s)
V	voltage (V)
We	Weber number = $\rho v^2 D/\sigma$ (-)
Wo	Womersley number = $(d/2) (2\pi f \rho_l/\mu_l)^{1/2}$ (-)
X	vapour quality = vapour mass fraction (-)
z	axial or vertical co-ordinate (m)
α	vapour/void fraction (volumetric) (-)
Δ	difference, drop (-)
δ	surface roughness (m)
ű	volume rate (m^3/s)
κ	thermal diffusivity (m^2/s)
ə	thermal conductivity (W/m.K)
μ	viscosity ($N.s/m^2$)
ν	angle (with respect to gravity) (rad)
π	dimensionless number (-)
ρ	density (kg/m^3)
σ	surface tension (N/m)

Subscripts

a	acceleration, adiabatic, axial
ch	capillary channel
C	cold
c	condenser
cool	coolant
e	evaporator
eff	effective
el	electric
f	friction
g	gravitation
H, h	hot
I	inner
l	liquid
m	momentum
max	maximum
M	model
ȝ	reference, outer, horizontal
p	pore
P	prototype
r	radial, or radius (m)
rad	radiation
s	entropy
t	total
tp	two-phase
v	vapour
w	water